We are IntechOpen, the world's leading publisher of Open Access books Built by scientists, for scientists

6,900
Open access books available

185,000
International authors and editors

200M
Downloads

Our authors are among the

154
Countries delivered to

TOP 1%
most cited scientists

12.2%
Contributors from top 500 universities



WEB OF SCIENCE™

Selection of our books indexed in the Book Citation Index in Web of Science™ Core Collection (BKCI)

Interested in publishing with us?
Contact book.department@intechopen.com

Numbers displayed above are based on latest data collected.
For more information visit www.intechopen.com



Chapter 8

Decoupling Control and Soft Sensor Design for an Experimental Platform

Thamiles Rodrigues de Melo,
Nathália Arthur Brunet Monteiro, Danilo Pequeno,
Jaidilson Jó da Silva and José Sérgio da Rocha Neto

Additional information is available at the end of the chapter

http://dx.doi.org/10.5772/intechopen.75708

Abstract

This chapter presents the design and implementation of a decoupling control strategy for an experimental platform and pilot plant, dedicated to the study of the fouling phenomena which occur in industrial tubes. Initially, a set of tests was done for the identification and validation of FOPDT models suitable to the four processes of the multivariable system: flow-voltage, flow-current, pressure-voltage, and pressure-current. After, the interaction between the inputs and outputs of the system was analyzed by the RGA and RNGA matrices. The static decoupling and decentralized PID controllers tuned by the Ziegler-Nichols and IMC methods were designed. Then, the set point tracking response was simulated and implemented using MATLAB and LabVIEW software, respectively. Finally, the concept of soft sensor was applied to monitor the output variables of the experimental platform, for a better performance of the decoupling control.

Keywords: multivariable system, FOPDT process, PID control, decoupling, soft sensor

1. Introduction

Automatic control arose from the need to improve performance of the systems, in search of better products at lower costs, and has made great advances in engineering, becoming of great importance in industrial processes. The increase in the complexity of the systems and the high level of automation present in the most diverse areas of the productive sectors has indicated the need to develop more precise and robust models, in order to make processes more reliable and to reduce the operating costs [1].

IntechOpen

© 2018 The Author(s). Licensee IntechOpen. This chapter is distributed under the terms of the Creative Commons Attribution License (http://creativecommons.org/licenses/by/3.0), which permits unrestricted use, distribution, and reproduction in any medium, provided the original work is properly cited. CC BY

In general, industrial processes have a multivariable nature, with multiple inputs and outputs, which configure multi-input multi-output (MIMO) systems. If these processes have two inputs and two outputs, then they can be referred to as two-input two-output (TITO) systems. Besides, many MIMO systems are treated as several TITO subsystems in practice [2].

Multivariable systems are more difficult to control due to interactions between input and output variables on each control loop. Thus, many problems associated with multivariable control are solved by means of the application of decentralized control theory. In this type of control, design techniques for single-input single-output (SISO) control systems are used in the pairing of manipulated variables (i.e., plant input signals on control) and process variables (i.e., output signals of the plant on control) [3, 4].

When the interactions between the control loops are not so significant, a diagonal controller (decentralized control) may be sufficient to guarantee control of the system. However, if the interactions are more significant, a complete matrix controller (centralized control) is more appropriate. One of the strategies for implementing centralized control is the use of decoupling devices together with a decentralized controller. Furthermore, the decoupling in a MIMO control system also allows the application of SISO control techniques, such as the proportional-integral-derivative (PID) controller tuning methods [5, 6].

The main advantage of PID control in industry can be attributed by the simplicity and ease of implementation for robustness over a wide range of operating conditions. The PID structure has three elements: a proportional term to close the feedback loop, an integral term to assure zero error to constant reference and disturbance inputs, and a derivative term to improve or realize the stability and good dynamic response. The preference for using the time constants of this controller in the industry refers to the physical meaning given to the operator on the system behavior to be controlled [7].

The task of a control system is to ensure the stability of the process, to minimize the influence of disturbances, and to optimize the overall performance. Thus, the industrial processes are instrumented with a large number of sensors. The purpose of sensors is to acquire data of the system. Currently, soft sensors have been used in industries to make physical systems meet the specifications of performance previously established with success, such as reconstructing the missing measurements during the operating of process and assisting in monitoring, control, and optimization of plant [8].

The soft sensors can be considered as the result of the intersection of the techniques of system modeling and identification and the intelligent instrument technology, instruments that, combined with digital systems like microprocessors or microcontrollers, modify their behavior, manipulating computationally the information to adapt to the collection and manipulation of the process data and transmitting them in the best possible way. The term “soft sensor” is a combination of the words “software” and “sensors,” because the models are usually a set of software routines and represent similar measurements of the real sensors [9].

Specific modeling techniques for soft sensors using artificial neural networks (ANNs) constitute an interesting development to be searched. This study has led to the interest in the development of soft sensors, using a computer program; the variables are estimated from the information collected by other measurements, without the industrial process being paralyzed.

In this context, the aim of this chapter is the design and implementation of a decoupling control strategy for an experimental platform dedicated to study the fouling phenomena. Besides, the concept of soft sensor allied to neural networks is applied to start the output variable monitoring of the platform, for a better performance of the decoupling control.

This chapter is structured as follows. Section 2 presents the basic concepts of MIMO control system using decoupling. Section 3 describes the experimental platform under study. Section 4 presents the methodology used for modeling and control of the system. Section 5 discusses the results obtained. Section 6 presents the special topic on an application of soft sensor for the closed-loop control. Section 7 summarizes a conclusion about the implementation.

2. Fundamentals of multivariable control systems

Multivariable systems, also called MIMO systems, are systems that have more than one input variable and more than one output variable. The main difference between a SISO system and a MIMO system is the presence of combinations (or directions) in the system.

The combinations are present in vectors and matrices, which compose the MIMO systems, but are not in scalars, that characterize the SISO systems, as observed in **Figure 1**. However, ideas and techniques applied to SISO systems can be extended to multivariable systems [10].

Consider a multivariable system with m inputs $u(t)$ and n outputs $y(t)$ in the time domain. The matrix representation of the system in the Laplace s domain is given according to Eq. (1):

$$\mathbf{Y}(s) = \mathbf{G_p}(s)\mathbf{U}(s) \Rightarrow \begin{bmatrix} Y_1(s) \\ Y_2(s) \\ \vdots \\ Y_n(s) \end{bmatrix} = \begin{bmatrix} G_{p_{11}}(s) & G_{p_{12}}(s) & \cdots & G_{p_{1m}}(s) \\ G_{p_{21}}(s) & G_{p_{22}}(s) & \cdots & G_{p_{2m}}(s) \\ \vdots & \vdots & \ddots & \vdots \\ G_{p_{n1}}(s) & G_{p_{n2}}(s) & \cdots & G_{p_{nm}}(s) \end{bmatrix} \cdot \begin{bmatrix} U_1(s) \\ U_2(s) \\ \vdots \\ U_m(s) \end{bmatrix} \quad (1)$$

where $\mathbf{Y}(s)$ is the output vector representing a set of process variables $Y_1(s)$, $Y_2(s)$, …, $Y_n(s)$, with order $n \times 1$; $\mathbf{U}(s)$ is the input vector representing a set of manipulated variables $U_1(s)$, $U_2(s)$, …, $U_m(s)$, with order $m \times 1$; and $\mathbf{G_p}(s)$ is the transfer function matrix of the plant, with order $n \times m$.

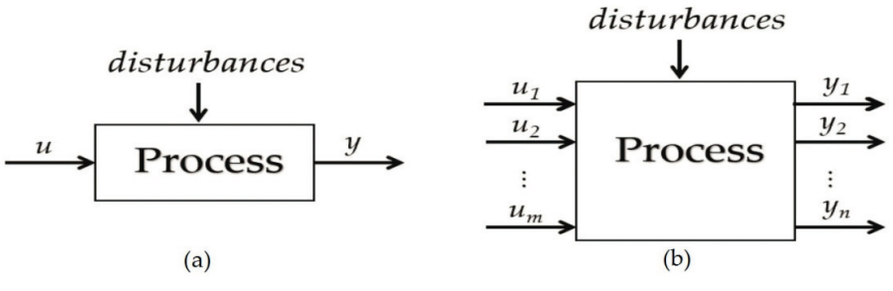


Figure 1. Block diagrams for (a) SISO and (b) MIMO systems. *Source*: Own author (2018).

In the multivariable system, if one of the inputs is modified and this affects the other outputs, then there is an *interaction* between the inputs and the outputs of the system. The interaction determines the level of coupling of the multivariable system, which can be:

- *Poorly coupled or uncoupled*, when u_1 only affects y_1, u_2 only affects y_2, and so on.
- *Strongly coupled*, when the change in u_i, with $i = 1, \ldots, m$, affects all outputs of the system, i.e., $y_1, y_2, \ldots, y_n$. If the effect of the manipulated variable is greater than the others in the plant, then the coupling has dominance in the system [11].

Thus, a *multivariable control system* can be treated as a control system that involves several manipulated and process variables to reduce the interferences caused by the interaction between the control loops. A feedback control loop for a MIMO system is observed in **Figure 2**, where $e(t)$ is the error between the output $y(t)$ and the reference $y_r(t)$.

When the elements outside the diagonal of the plant matrix are elevated, one type of MIMO control strategy denominated as *decoupling control* has the ability to removing the interactions between two or more variables. For example, the decoupling configuration of a TITO system with decentralized control is observed in **Figure 3**. The process variable $\mathbf{Y}(s) = [Y_1(s) \;\; Y_2(s)]^T$ tracks the set point $\mathbf{Y_r}(s) = [Y_{r_1}(s) \;\; Y_{r_2}(s)]^T$ by means of the control strategies implemented in the decentralized controller matrix $\mathbf{G_c}(s)$. Furthermore, this matrix produces the manipulated variable $\mathbf{U}(s) = [U_1(s) \;\; U_2(s)]^T$ to actuate in the plant matrix $\mathbf{G_p}(s)$.

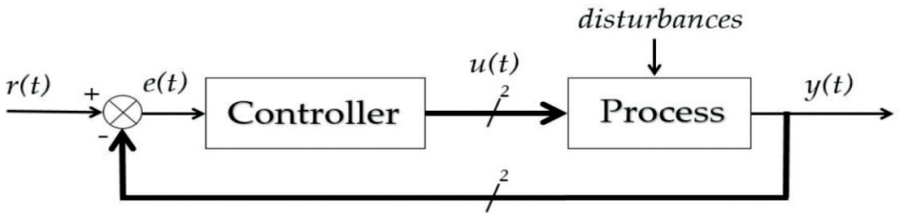


Figure 2. General structure of a feedback control loop for a MIMO system. *Source*: Own author (2018).

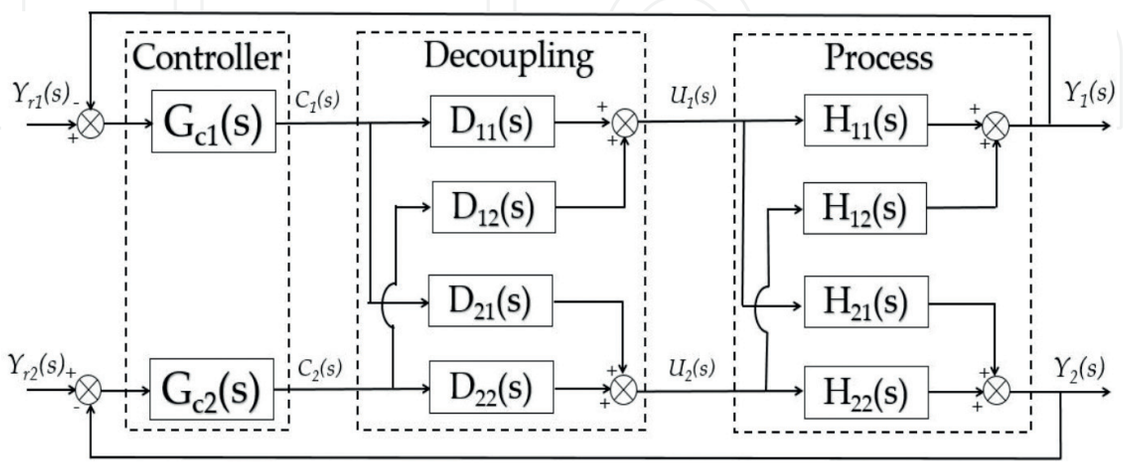


Figure 3. The decoupling configuration of a TITO system. *Source*: Own author (2018).

For a TITO system, the plant matrix $\mathbf{G_p}(s)$ can be expressed by Eq. (2):

$$\mathbf{G_p}(s)=\begin{bmatrix} G_{p_{11}}(s) & G_{p_{12}}(s) \\ G_{p_{21}}(s) & G_{p_{22}}(s) \end{bmatrix}=\begin{bmatrix} \frac{Y_1(s)}{U_1(s)} & \frac{Y_1(s)}{U_2(s)} \\ \frac{Y_2(s)}{U_1(s)} & \frac{Y_2(s)}{U_2(s)} \end{bmatrix} \tag{2}$$

where $G_{p_{ij}}(s)$, with i, j ranging from 1 to 2, is the transfer function of each SISO process in the Laplace domain, resulting from possible input-output combinations in a TITO system.

Since the decentralized controller matrix $\mathbf{G_c}(s)$ has order compatible with the plant matrix $\mathbf{G_p}(s)$, then it can be expressed according to Eq. (3):

$$\mathbf{G_c}(s)=\begin{bmatrix} G_{c_1}(s) & 0 \\ 0 & G_{c_2}(s) \end{bmatrix} \tag{3}$$

where $G_{c_i}(s)$, with i varying from 1 to 2, is the transfer function of the implemented controller in the decentralized control structure in the Laplace domain.

If the interaction between the inputs and outputs was poorly coupled, then the output $\mathbf{C}(s)$ of the decentralized controller equals the manipulated variable $\mathbf{U}(s)$. Otherwise, if necessary to apply the decoupling on the system, then the controller output and the plant input are distinct by means of the design of the decoupling matrix $\mathbf{D}(s)$, as represented in Eq. (4):

$$\mathbf{U}(s)=\mathbf{D}(s)\mathbf{C}(s)\Rightarrow\begin{bmatrix} U_1(s) \\ U_2(s) \end{bmatrix}=\begin{bmatrix} D_{11}(s) & D_{12}(s) \\ D_{21}(s) & D_{22}(s) \end{bmatrix}\cdot\begin{bmatrix} C_1(s) \\ C_2(s) \end{bmatrix} \tag{4}$$

When replacing Eq. (4) in Eq. (1), considering this matrix with compatible order to the TITO system, the resulting matrix $\mathbf{T}(s)$ is obtained with the decoupling, as represented in Eq. (5):

$$\mathbf{Y}(s)=\mathbf{G_p}(s)\mathbf{U}(s)=\mathbf{G_p}(s)\mathbf{D}(s)\mathbf{C}(s)\Rightarrow\mathbf{Y}(s)=\mathbf{T}(s)\mathbf{C}(s) \tag{5}$$

In this case, the resulting matrix becomes diagonal and represents the desired dynamic for the decoupled TITO system [12], according to Eq. (6):

$$\mathbf{T}(s)=\mathbf{G_p}(s)\mathbf{D}(s)\Rightarrow\begin{bmatrix} T_{11}(s) & 0 \\ 0 & T_{22}(s) \end{bmatrix}=\begin{bmatrix} G_{p_{11}}(s) & G_{p_{12}}(s) \\ G_{p_{21}}(s) & G_{p_{22}}(s) \end{bmatrix}\cdot\begin{bmatrix} D_{11}(s) & D_{12}(s) \\ D_{21}(s) & D_{22}(s) \end{bmatrix} \tag{6}$$

Therefore, the product of the inverse of plant matrix with the resulting matrix obtains the decoupling matrix, according to Eq. (7):

$$\mathbf{D}(s)=\mathbf{G_p}(s)^{-1}\mathbf{T}(s)=\frac{1}{G_{p_{11}}(s)G_{p_{22}}(s)-G_{p_{12}}(s)G_{p_{21}}(s)}\cdot\begin{bmatrix} G_{p_{22}}(s)T_{11}(s) & -G_{p_{12}}(s)T_{22}(s) \\ -G_{p_{21}}(s)T_{11}(s) & G_{p_{11}}(s)T_{22}(s) \end{bmatrix} \tag{7}$$

For a simulation example on MIMO system, consider a Luyben and Vinnate distillation column model, cited in [13], with diagonal pairing ($y_1 - u_1$ /$y_2 - u_2$), is given by Eq. (8).

$$\mathbf{G_p}(s)=\begin{bmatrix} \dfrac{-2.16}{8s+1}e^{-s} & \dfrac{1.26}{9.5s+1}e^{-0.3s} \\ \dfrac{-2.75}{9.5s+1}e^{-1.8s} & \dfrac{4.28}{9.2s+1}e^{-0.35s} \end{bmatrix} \tag{8}$$

The static decoupling matrix $\mathbf{D}(s)$ is given by Eq. (9):

$$\mathbf{D}(j0) = \begin{bmatrix} 1 & 0.5833 \\ 0.6425 & 1 \end{bmatrix} \tag{9}$$

The set point tracking response of the control loops simulated by means of MATLAB software is shown in **Figure 4**, using the PI controllers tuned by Internal Model Control (IMC) method (better explained in Section 4), according to **Table 1**.

After the basic concepts of a multivariable control system, the description of the plant under test and the formulation of the control problem are shown in Section 3.

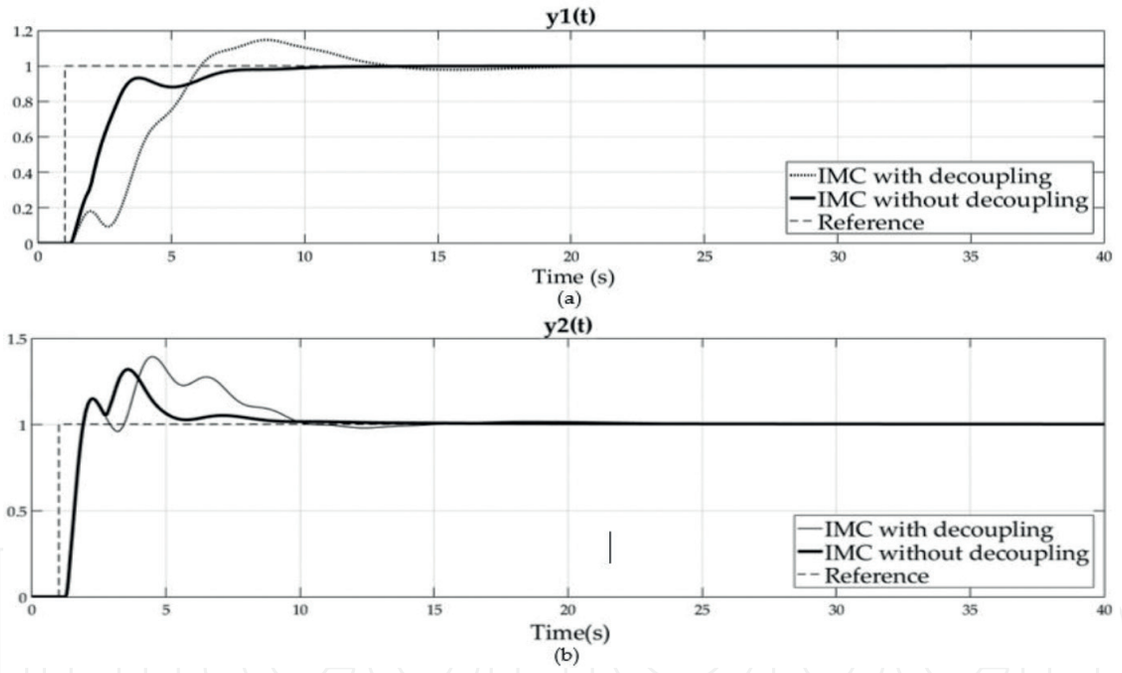


Figure 4. The simulation of set-point tracking response: (a) the flow and (b) pressure control loops with static decoupling – ZN and IMC methods. *Source*: Own author (2018).

Tuning method	Process	Controller	$K_{P_{in}}$	$T_{I_{in}}$
IMC	11	$G_{c1}(s)$	−3.9352	8.5000
	22	$G_{c2}(s)$	6.2583	9.3750

Source: Own author (2018).

Table 1. PID controllers obtained with IMC tuning method.

3. Experimental platform

To study the process of fouling formation in industrial tubes, an experimental platform was built in the Laboratory of Electronic Instrumentation and Control (LIEC) of the Electrical Engineering Department at Federal University of Campina Grande, Brazil.

The experimental platform shown in **Figure 5** is characterized as a distributed monitoring of fluid transport system with galvanized iron tubes of different diameters (1″, 1 1/2″, 2″). The 2″ tubes are assumed as the main tube, and the other tubes are used for generation of disturbances in the system.

For the monitoring and control of the phenomena in study, three flow sensors and three pressure sensors were chosen, which were fixed in each type of tube and one temperature sensor which was submerged in the fluid (in this case, the water) stored in a 100 liter tank. Besides, on the experimental platform, there is one control valve with electric actuator and two manual valves for outflow control, even as one frequency inverter used for the rotate velocity control of the water pump.

Furthermore, there is one programmable logic controller (PLC) responsible by the integration between sensors, actuators, and computer on the experimental platform. The sensors communicate with the PLC via 4–20 mA standard, and the actuators communicate with controller using the 4–20 mA or 0–10 V standard.

To determine the control structure for the experimental platform considering as a TITO system, the following definitions were done [14]:

- The $U_1(s)$ and $U_2(s)$ represent the voltage signal $V(s)$ and the current signal $I(s)$ applied on the actuators of the experimental platform, i.e., the frequency inverter and the control valve.

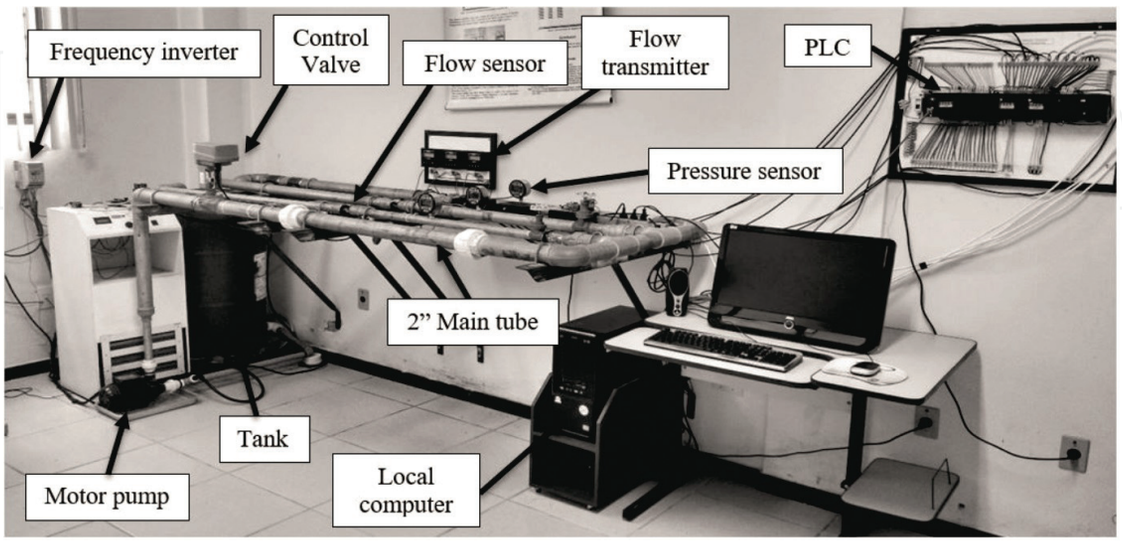


Figure 5. Photograph of experimental platform in study. *Source*: Own author (2018).

- The $Y_1(s)$ and $Y_2(s)$ represent the flow measure $Q(s)$ and the pressure measure $P(s)$ monitored by means of the flow and pressure sensors in the main tube.
- The $Y_{r_1}(s)$ and $Y_{r_2}(s)$ represent the reference flow $Q_r(s)$ and the reference pressure $P_r(s)$ which will be adopted for operating in the main tube.

In the implementation of the control structure proposed for the experimental platform, it is necessary that:

- The plant operates in the percentage range of the reference values, in order to minimize the unplanned interventions resulting from the fouling phenomena.
- The conditions of the multivariable control system do not exceed the operating limits of the plant, such as the measurements made by the flow sensors and pressure and the actuations performed by the frequency inverter and control valve within the full-scale range of these transducers.

The methodology adopted for the development of a decoupling control on the experimental platform is discussed in Section 4.

4. System modeling, interaction analysis, and control design

The plant matrix $\mathbf{G_p}(s)$ in the experimental platform is composed of four processes: $G_{p_{11}}(s)$ representing the flow-voltage process, $G_{p_{12}}(s)$ representing the flow-current process, $G_{p_{21}}(s)$ representing the pressure-voltage process, and $G_{p_{22}}(s)$ representing the pressure-current process. In this work, each transfer function $G_{p_{ij}}(s)$ is assumed as a first-order plus dead time (FOPDT) process, according to Eq. (10):

$$G_{p_{ij}}(s) = \frac{K_{ij}e^{-L_{ij}s}}{\tau_{ij}s + 1} \tag{10}$$

where K_{ij} is the gain of the process [dimensionless], L_{ij} is the dead time [s], and τ_{ij} is the time constant of FOPDT process [s].

For the identification of the models experimentally, the behavior of the output signals is observed by means of the application of known input signals in each process. In practice, consecutive tests are done on the system, and the input and output data are stored. Then, these data are processed in a specific software to adjust the experimental curves obtained to the known theoretical models. At last, the model obtained is valid for each process.

Thus, these tests were executed in the four processes of the system. All FOPDT process models were obtained individually from the experiments based on the critical point of the plant, which consists in the application of consecutive switches in the manipulated variable in a determined time interval, taking into account the dynamics of the system. At the end of the switches, the application of a pulse was executed. Subsequently, the parameters of each FOPDT process

model were estimated and validated by means of a software developed in C#, better described in Barros et al. [15], in which the frequency response method was used as the identification method and Theil coefficient as validation method.

The standard coefficient U, proposed by Theil [16], can be interpreted as the division of the root mean square error (RMSE) of the proposed prediction for the variable, by the RMSE value of the original variable, as expressed by Eq. (11):

$$U = \frac{\sqrt{\frac{1}{N}\sum_{t=1}^{N}\left(\widehat{y}(t) - y(t)\right)^2}}{\sqrt{\frac{1}{N}\sum_{t=1}^{N}\widehat{y}^2(t)} + \sqrt{\frac{1}{N}\sum_{t=1}^{N}y^2(t)}} \tag{11}$$

where $\widehat{y}(t)$ is the predicted (estimated) value, $y(t)$ is the observed (measured) value, and N is the number of measurements.

If U equals 1, it means that the proposed model is as good as the real system. If U is greater than 1, the predicted model should be discarded. Thus, the coefficient U should only be considered when it is greater than 0 and less than 1, indicating a greater accuracy of the obtained model. When U is closer to 0, the prediction should be improved [17].

To determine the best loop pairing in the control structure, the Relative Gain Array (RGA) and Relative Normalized Gain Array (RNGA) matrices were calculated, as proposed by Bristol [18] and He et al. [19], respectively. The RGA matrix only requires information on the steady-state system to measure the process interactions and thus to recommend on the most efficient parity. In this way, the elements of RGA matrix are dependent on the steady-state system gains, according to Eq. (12):

$$\mathbf{\Lambda} = \mathbf{K} \otimes \mathbf{K}^{-\mathbf{T}} \tag{12}$$

where $\mathbf{K}=\mathbf{G_p}(j0)$, with $K_{ij} = G_{p_{ij}}(j0)$ being the steady-state gain, and $\otimes$ denotes element-by-element multiplication.

For a TITO system, the corresponding RGA matrix can be calculated from Eq. (13):

$$\mathbf{\Lambda} = \begin{bmatrix} \lambda_{11} & \lambda_{12} \\ \lambda_{21} & \lambda_{22} \end{bmatrix} = \begin{bmatrix} \lambda_{11} & 1-\lambda_{11} \\ 1-\lambda_{11} & \lambda_{11} \end{bmatrix} \tag{13}$$

where $\lambda_{11} = \frac{1}{1-\kappa}$, with $\kappa = \frac{K_{21}K_{12}}{K_{11}K_{22}}$ being the interaction coefficient.

The correct interpretation of the elements of the RGA matrix allows quantifying the interaction measure involved in all the possible control configurations of a $N \times N$ system. Thus, it is recommended to choose the control configuration that has the least interaction as follows:

i. Choose the control configuration with the diagonal or off-diagonal elements λ_{ij} as close to 1.

ii. If possible, avoid to choose a control configuration where $\lambda_{ij} >> 1$.

iii. Settings with $\lambda_{ij} < 0$ are totally undesirable, because the negative values indicate the possibility of a closed-loop unstable.

In order to overcome the deficiency of the RGA method of not including the dynamic behavior, the RNGA matrix was used. In this matrix, steady-state behavior can be easily characterized by the matrix **K,** whereas dynamic behavior can be obtained by the response time of the process variable relative to the manipulated variable.

Thus, the RNGA matrix is defined in Eq. (14), and it depends of the normalized gain matrix $\mathbf{K_N}$, which considers both characteristics mentioned above. Similar to RGA matrix, the best loop pairing is chosen when the diagonal or off-diagonal elements ϕ_{ij} are close to 1:

$$\mathbf{\Phi} = \mathbf{K_N} \otimes \mathbf{K_N^{-T}} \tag{14}$$

where $\mathbf{K_N}$=$\mathbf{G_p}(j0) \odot \mathbf{T_{ar}}$, with $k_{Nij} = \frac{G_{p_{ij}}(j0)}{\tau_{ar\,ij}}$ being the normalized gain, where $G_{p_{ij}}(j0)$ is the steady-state gain and $\tau_{ar\,ij}$ is the mean residence time, which is an indicator of the speed of the response of y_i given the action of u_j, and $\odot$ being the element-by-element division.

Once loop pairing has been defined, the decoupling matrix $\mathbf{D}(s)$ was calculated using the static decoupling. This type of decoupling allows the resulting matrix $\mathbf{T}(s)$ to be diagonal at steady state, i.e., only $s = j0$. In the case of a TITO system, the static decoupled matrix can be given according to Eq. (15):

$$\mathbf{D}(j0) = \begin{bmatrix} 1 & -\dfrac{G_{p_{12}}(j0)}{G_{p_{11}}(j0)} \\ -\dfrac{G_{p_{21}}(j0)}{G_{p_{22}}(j0)} & 1 \end{bmatrix} = \begin{bmatrix} 1 & -\dfrac{K_{12}}{K_{11}} \\ -\dfrac{K_{21}}{K_{22}} & 1 \end{bmatrix} \tag{15}$$

For closing the control loop proposed, the elements of decentralized controller matrix $\mathbf{G_c}(s)$ were obtained by means of the PID theory, which combines proportional, integral, and derivative actions to control each process, as expressed by Eq. (16):

$$G_{c_i}(s) = K_{P_i}\left(1 + \frac{1}{T_{I_i}s} + T_{D_i}s\right) \tag{16}$$

where K_{P_i} is the proportional gain [dimensionless], T_{I_i} is integral time constant [s], and T_{D_i} is the derivative time constant [s].

To calculate the parameters for each decentralized controller $G_{c_i}(s)$, the PID tuning methods were applied on the control structure proposed. The tuning method proposed by Ziegler and Nichols [20] determines that the controller parameters are obtained from the time response of the process to be controlled. Thus, for a FOPDT process model, the PID controller parameters can be calculated with the Ziegler-Nichols (ZN) method according to **Table 2**.

Other PID tuning methods originally proposed by Garcia and Morari [21] consider the process model as an integral part of the controller. The central idea of the Internal Model Control (IMC)

method is that the controller can be obtained only if the control system incorporates, explicitly or implicitly, some representation of the process to be controlled.

For a FOPDT process model, this method considers that the dead time process can be approximated using the *first-order Padé approximation*. Besides, the general form of the PID controller tuned by the IMC method has a low pass filter with a filtering component τ_c, which is used precisely to decrease the sensitivity to modeling errors [22]. The calculation of PID controller parameters can be calculated according to **Table 3**.

At last, to evaluate the output control performance, the Integral Absolute Error (IAE) and Integral Squared Error (ISE) metrics were used as quantitative performance measures, according to Eqs. (17) and (18), respectively:

$$\text{IAE} = \int_0^T |e(t)|dt \tag{17}$$

$$\text{ISE} = \int_0^T e^2(t)dt \tag{18}$$

where T = t_s, which is the settling time of the system.

With all the necessary parameters obtained, the decoupling control was simulated in the MATLAB software and implemented using a Human Machine Interface (HMI) developed in the LabVIEW software. For the system test, 20 liters per minute (LPM) was used as flow set point and 40 mBar as pressure set point, according to the turbulent flow regime of the experimental platform proposed in Melo et al. [23].

The results obtained on the development of the decoupling control are shown in Section 5.

Controller	**Parameters**		
$G_{c_i}(s)$	K_{P_i}	T_{I_i}	T_{D_i}
PID	$\frac{1.2\tau_{ij}}{K_{ij}L_{ij}}$	$2L_{ij}$	$\frac{L_{ij}}{2}$

Source: Own author (2018).

Table 2. PID tuning by the ZN method.

Controller		**Parameters**	
$G_{c_i}(s)$	K_{P_i}	T_{I_i}	T_{D_i}
PID	$\frac{2\tau_{ij}+L_{ij}}{K_{ij}\left(\tau_c+L_{ij}\right)}$	$\tau_{ij}+\frac{L_{ij}}{2}$	$\frac{\tau_{ij}L_{ij}}{2\tau_{ij}+L_{ij}}$

Source: Own author (2018).

Table 3. PID tuning by the IMC method.

5. Results and discussion

The actual response curve of the flow-voltage process is shown in **Figure 6a**, while the comparative of the responses curve between the identified mathematical model and the experimental model of the process is shown in **Figure 6b**. Similar results were obtained for other processes of the plant matrix, thus validating the mathematical models identified. Besides, the input and output signals in this figure are represented as words on a decimal basis of the analog-to-digital converter (ADC) on the PLC, which can be converted in the measuring units by means of the equivalence relations in the HMI.

The obtained models were approximated by FOPDT process model with sufficient dead time to reliably model the system in question. Among the models obtained using the software developed in C#, the best models that were chosen according to the Theil coefficient criterion are shown in **Table 4**.

From these models, the best loop pairing present in the system was defined according to the RGA and RNGA matrices obtained, as expressed in Eqs. (19) and (20), respectively:

$$\mathbf{\Lambda} = \begin{bmatrix} -1.9116 & 2.9116 \\ 2.9116 & -1.9116 \end{bmatrix} \tag{19}$$

$$\mathbf{\Phi} = \begin{bmatrix} -4.1699 & 5.1699 \\ 5.1699 & -4.1699 \end{bmatrix} \tag{20}$$

Based on the elements of both matrices, it can be observed that the loop pairing suggested to control the TITO system in study is the off-diagonal pairing, i.e., $y_1 - u_2 / y_2 - u_1$. Therefore, the flow variable must be controlled by the current signal, applied to the control valve, while the pressure variable must be controlled by voltage applied to the frequency inverter.

After the choice of the best loop pairing for the control loops, the static decoupling matrix was calculated, as expressed in Eq. (21). The objective of the decoupling is to make the decentralized controllers operate on two independent processes in control loops: pressure-voltage and flow-current. Therefore, to ensure the correctness of operating the decoupling control, the processes associated to both control loops were reallocated for diagonal elements of the plant matrix:

$$\mathbf{D}(j0) = \begin{bmatrix} 1 & -0.7276 \\ -0.9023 & 1 \end{bmatrix} \tag{21}$$

Besides, the decentralized controllers were designed for the selected control loops. The controller parameters obtained by tuning methods described are shown in **Table 5**. For the calculation of the filtering component τ_c in the IMC method, this work proceeded according to Skogestad [24].

The set point tracking response of the flow and pressure control loops simulated by means of MATLAB software is shown in **Figure 7**, using the PID controllers tuned by the Ziegler-Nichols and IMC methods with static decoupling. In this case, the choice of τ_c leads to

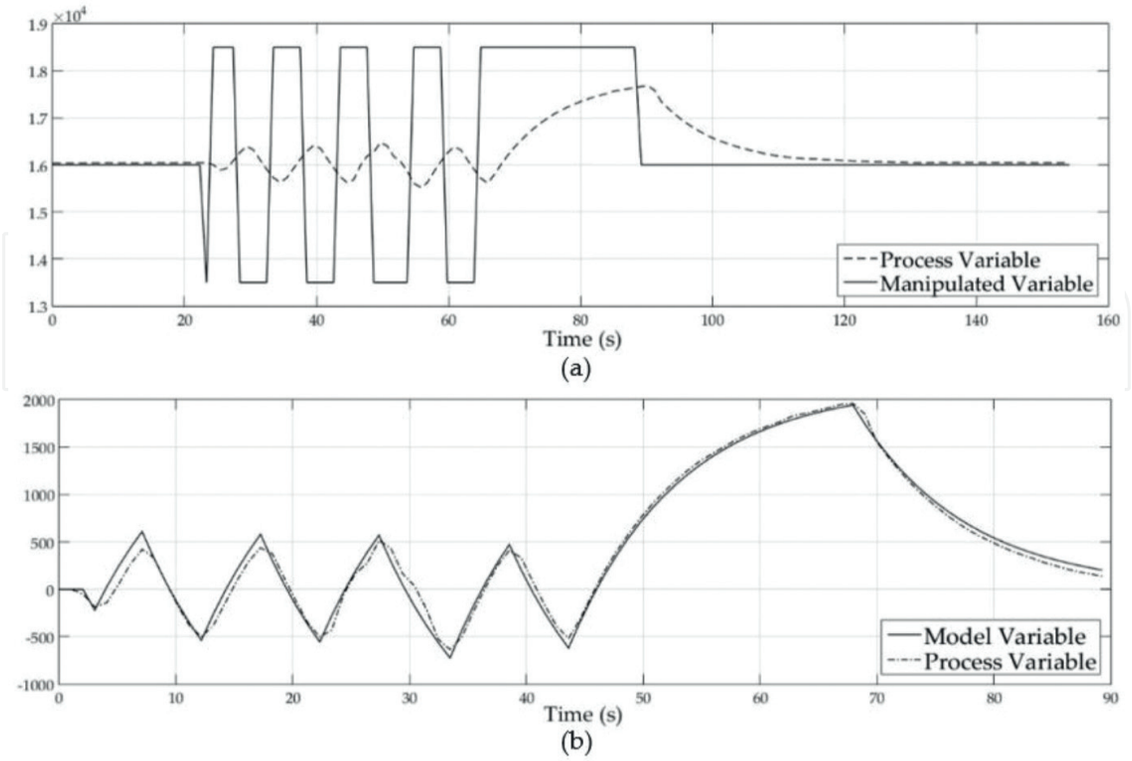


Figure 6. System modeling: (a) the response curve of the flow-voltage process and (b) the response curve of the identified model and the experimental model. *Source*: Own author (2018).

aggressive control action, principally to compensate the sluggish dynamic of the flow-current process.

In order to compare the output control performance of both PID tuning methods, the ISE and IAE metrics were used. The values obtained for these metrics are shown in **Table 6**. According to these performance metrics, it was verified that the strategy of control with the lowest values was the IMC controller for both control loops used.

The set point tracking response of the flow and pressure control loops on the experimental platform, supervised by the HMI developed in LabVIEW software, is shown in **Figure 8**, using the PID controllers tuned by the ZN and IMC methods with static decoupling.

Process	**Transfer function**	**U**
Flow-voltage	$G_{p_{11}}(s) = \frac{0.8622}{9.9680s+1} e^{-8.2500s}$	0.0448
Pressure-voltage	$G_{p_{21}}(s) = \frac{0.0469}{5.2040s+1} e^{-10.0100s}$	0.1119
Flow-current	$G_{p_{12}}(s) = \frac{1.1850}{18.7900s+1} e^{-6.0840s}$	0.0660
Pressure-current	$G_{p_{22}}(s) = \frac{0.0423}{10.8200s+1} e^{-6.0840s}$	0.0796

Source: Own author (2018).

Table 4. FOPDT process models obtained experimentally.

Tuning method	Process	Controller	$K_{P_{in}}$	$T_{I_{in}}$	$T_{D_{in}}$
ZN	Pressure-voltage	$G_{c_1}(s)$	0.6239	20.0200	5.0050
	Flow-current	$G_{c_2}(s)$	3.7061	12.1680	3.0420
IMC	Pressure-voltage	$G_{c_1}(s)$	14.4972	10.2090	2.5513
	Flow-current	$G_{c_2}(s)$	2.0188	21.8320	2.6181

Source: Own author (2018).

Table 5. PID controllers obtained with both tuning methods.

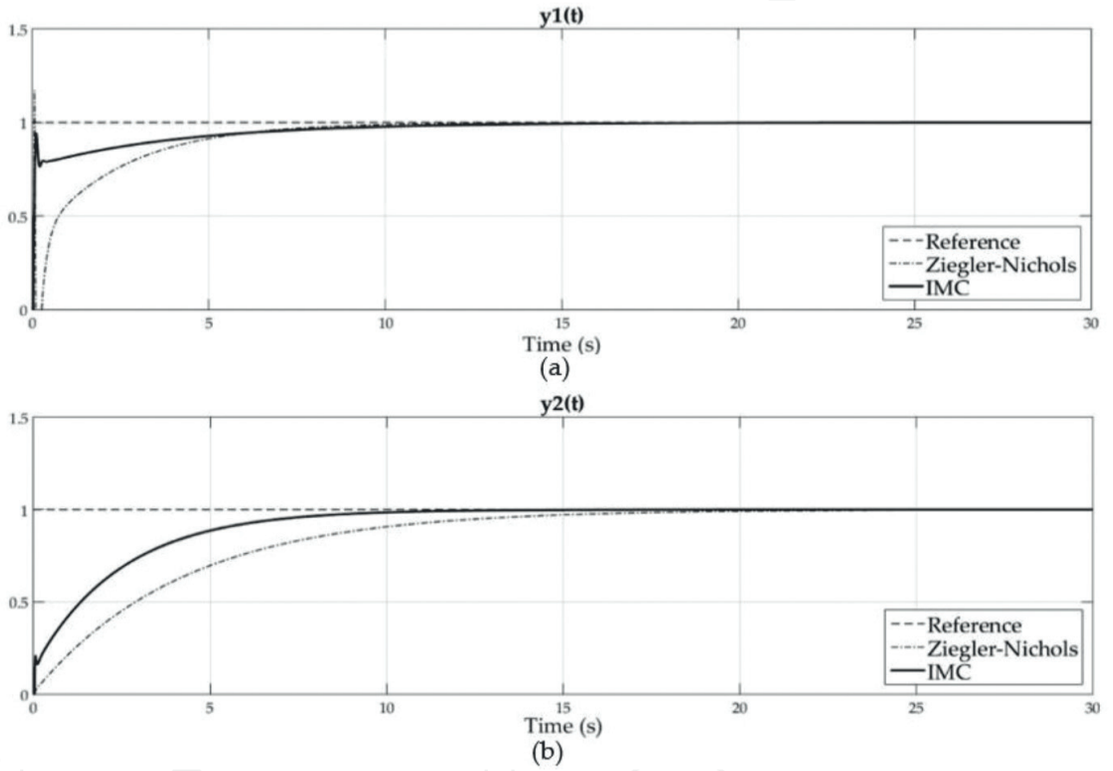


Figure 7. The simulation of set-point tracking response: (a) the flow and (b) pressure control loops with static decoupling – ZN and IMC methods. *Source*: Own author (2018).

Tuning method	Process	Controller	IAE	ISE
ZN	Pressure-voltage	$G_{c_1}(s)$	64.1477	46.7040
	Flow-current	$G_{c_2}(s)$	52.1777	42.4687
IMC	Pressure-voltage	$G_{c_1}(s)$	49.1532	34.0354
	Flow-current	$G_{c_2}(s)$	39.0924	28.9877

Source: Own author (2018).

Table 6. IAE and ISE performance metrics.

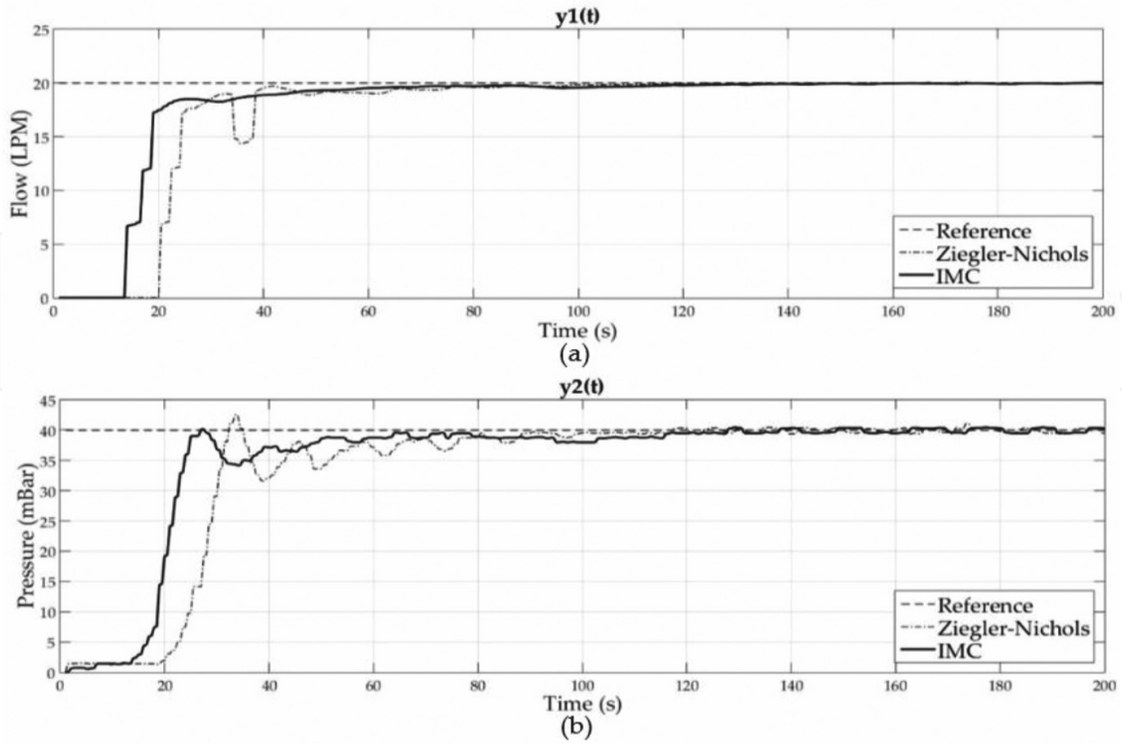


Figure 8. The implementation of set-point tracking response: (a) the flow and (b) pressure control loops on the experimental platform. *Source*: Own author (2018).

During the time interval around 30 s, it is observed that rapid pressure fluctuations in the system with ZN method resulted in flow reversals, i.e., a suction phenomenon was caused by the action opening of control valve, and this situation leads to an undesirable response in the closed-loop control. From the 140 s, both the process variables had already reached the steady state.

For the control system implemented to continue operating correctly, a good process instrumentation is fundamental. From this, the use of the soft sensor with the control system already designed with the objective of reducing the dependence of the physical sensors, as described in Section 6, is proposed.

6. Practical application of soft sensor

The concept of the use of the soft sensor aims at mathematical modeling of processes with focus on the prediction of the property, from available measurements of the other plant variables [25]. Mathematical models of processes designed to estimate relevant process variables to control can help to reduce the need for measuring devices, improve system reliability, and develop tight control policies. Thus, soft sensors offer a number of attractive properties to make the control process more reliable.

Irrespective of whether a maintenance intervention is programmed or accidental, the measuring hardware needs to be turned off and suitably substituted. The backup of measuring

instrumentation is a typical application of soft sensors. Thus, soft sensor is a mechanism used to replace the temporary or permanent unavailability of a physical sensor in a plant, which can happen due to the real sensor failure or removal for maintenance [26, 27].

For example, in the network scheme for a MIMO system as shown in **Figure 9**, the soft sensor running in parallel with the physical process is updated in real time with the same control signal data transmitted on the network to the actuators. When the physical sensor is not available for measurement, the switch at the sensor output changes from the position *P* to position *S* to get the output generated by the soft sensor [28].

The use of artificial intelligence techniques in the modeling of nonlinear dynamic systems has been diffused in the literature in recent years. This interest is motivated by the characteristics of these techniques that allow the development of models that are universal approximation of functions. In fact, depending on the technique, it is possible to approximate with arbitrary precision a continuous nonlinear function defined in a compact region (limited and closed) based on quantitative and qualitative information [29, 30].

Among the techniques of artificial intelligence used in the modeling of dynamic systems, artificial neural networks can be emphasized. The application of artificial neural networks in the prediction of variables can be auxiliary in the implementation of the soft sensor to process monitoring, in search of the processes with better performance and that are more reliable. Thus, the concept of soft sensor allied to ANNs is applied to start the output variables monitoring of the experimental platform.

On this platform, as mentioned in Section 3, there are two processes for monitoring and control which can be distinguished by the actuator element: valve position (current) or variation in the operation frequency of the motor pump (voltage). It is necessary to define a fixed operating point for one of the actuators. For example, in **Figure 10** the illustration of the inputs and outputs of the process can be observed, where, in the case 1, the position of the valve is fixed and the operation frequency of the motor pump is varied and, in the case 2, the motor pump working with fixed operating frequency is used and the position of the valve is varied, in both cases, to monitor and control the flow and pressure values in the tube.

Initially, to visualize a soft sensor working in the process, the monitoring of the flow values was done on the platform using a soft sensor designed by neural networks, with the fixed valve position, and varying the frequency (voltage) to pump the water inside the tube.

To test flow value monitoring, a frequency was applied to pump the water inside the tube, and the flow values measured and estimated (soft sensor) were observed. In a certain time, the flow

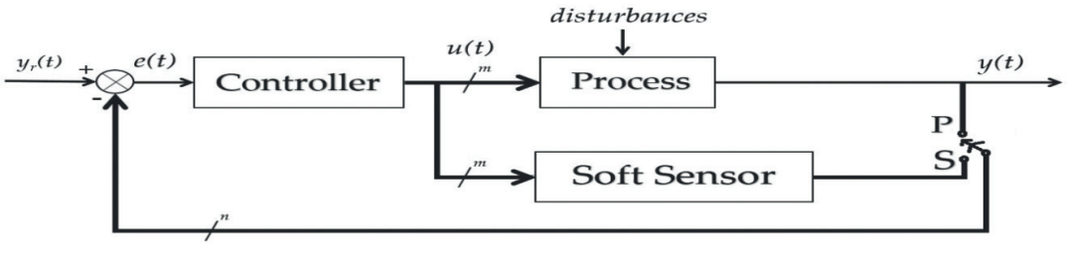


Figure 9. Feedback control loop with a soft sensor. *Source*: Own author (2018).

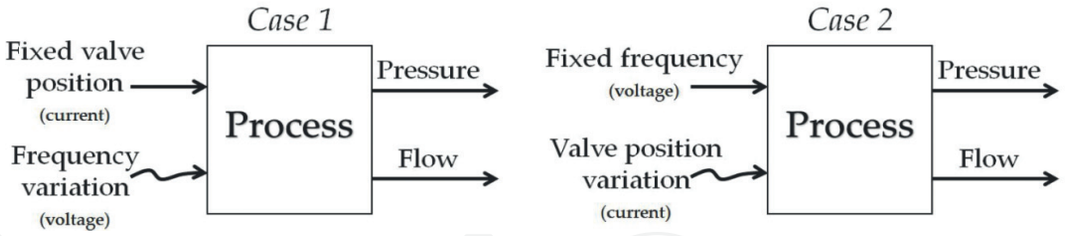


Figure 10. Operating point of the process for soft sensor design. *Source*: Own author (2018).

sensor was withdrawn, losing the measured signal by the real sensor. With the loss of the measured signal, to avoid stop the process, the neural network, based on the process input, estimates the flow value, so that the process can be monitored by continuing its operation, with the estimated values (soft sensor), while the real sensor signal is not recovered.

In **Figure 11**, the graph with the monitoring of the flow values as a function of time, for a better visualization of time duration of the transition from the estimated value response (soft sensor) to the measured real value, is observed. In the transition with the return of the real sensor signal, three samples were passed, lasting 3.39 seconds, which is the duration that the system worked without both signals, real and soft sensor. The purpose is a transition as short as possible, obtaining a process monitored for a longer time.

As presented, it was possible to estimate the flow values. In the case of the signal loss of the real sensor, it is possible to use the implemented soft sensor for monitoring of the process, avoiding unnecessary stopping. The conclusions obtained with this work and the perspectives for the improvement of the control system proposed are shown in Section 7.

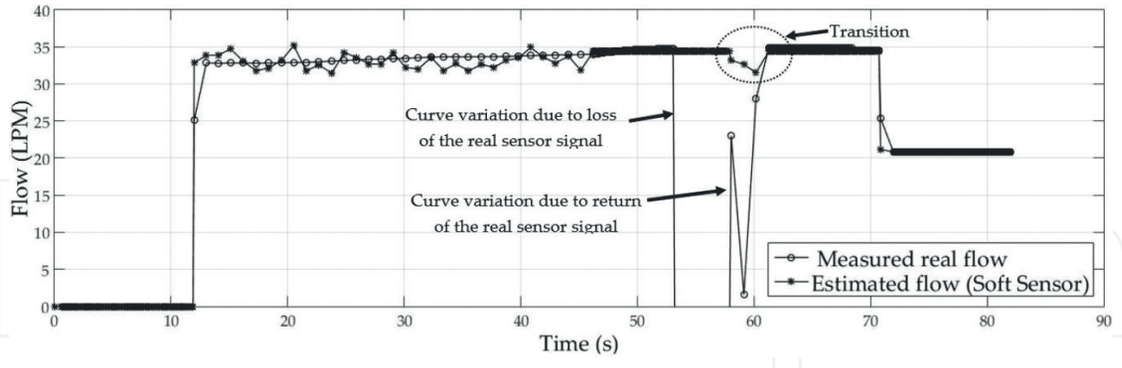


Figure 11. Flow variable monitoring in the MATLAB software. *Source*: Own author (2018).

7. Conclusion and future works

The present chapter consisted in the design and implementation of a decoupling control strategy for an experimental platform dedicated to study the fouling phenomena. This platform is considered as a TITO system, i.e., the voltage and current signals as the input system and the flow and pressure measurements as the output system.

Initially, a set of tests were done to identify FOPDT process models of the plant matrix, using the frequency response method for parameter estimation in each model and the Theil coefficients for the validation models. Then, the interaction between the inputs and outputs of the system was analyzed using RGA and RNGA matrices, which suggested the off-diagonal pairing as the best pairing loops, i.e., the flow-current and pressure-voltage processes for the closed-loop control.

Due to strong coupling loops, the static decoupling matrix was calculated, and finally the decentralized controller matrix was obtained using the ZN and IMC methods as PID tuning techniques. After the simulation and implementation of the decoupling control proposed, using MATLAB and LabVIEW software, respectively, the IAE and ISE performance metrics were calculated to analyze the output performance of the control loops.

Therefore, for the system under study, the best decoupling control strategy is associated with the IMC method. Even if the decoupling to be calculate for an exact mathematical model, the PID controllers obtained using this tuning method has the ability to ensure robust control against possible modeling errors.

For a better performance of the decoupling control, the soft sensor design was applied to start the output variable monitoring of the experimental platform. The general idea was to design a fully monitored process via computer program, so that if the measurement of the output variable fails for any reason, it is possible to use the soft sensor to infer the flow rate values (in this case, variable of interest in monitoring).

In the future works, it is possible to develop other soft sensors that will be integrated into the feedback control loop proposed to avoid interruptions performed to solve problems that could be solved without stopping the process. This makes the process more reliable, with better performance and with less difficulty to detect and solve possible failures.

Acknowledgements

The authors would like to thank CNPq and PPgEE-COPELE for financial support of project.

Author details

Thamiles Rodrigues de Melo[1]*, Nathália Arthur Brunet Monteiro[1], Danilo Pequeno[1], Jaidilson Jó da Silva[2] and José Sérgio da Rocha Neto[2]

*Address all correspondence to: thamiles.melo@ee.ufcg.edu.br

1 Post-Graduate Program in Electrical Engineering, PPgEE, COPELE, Federal University of Campina Grande (UFCG), Campina Grande, PB, Brazil

2 Department of Electrical Engineering (DEE), Federal University of Campina Grande (UFCG), Campina Grande, PB, Brazil

References

[1] Ogata K. Modern Control Engineering. 5th ed. São Paulo: Prentice Hall; 2009. 894 p. DOI: ISBN-10: 0136156738. ISBN-13: 978-0136156734

[2] Liu T, Zhang W, Danying G. Analytical multiloop PI/PID controller design for two-by-two processes with time delays. Industrial & Engineering Chemistry. 2005;**44**(6):1832-1841. DOI: 10.1021/ie0493715

[3] García MA, Salgado ME, Silva EI. Achievable performance bounds for tall MIMO systems. IET Control Theory & Applications. 2011;**5**(5):736-743. DOI: 10.1049/iet-cta.2010.0328

[4] Kookos IK, Lygeros AI. An algorithmic method for control structure selection based on the RGA and RIA interaction measures. Chemical Engineering Research and Design. 1998;**76**(4):458-464. DOI: 10.1205/026387698525072

[5] Garrido J, Vázquez F, Morilla F. Generalized inverted decoupling for TITO processes. In: Proceedings of the 18th International Federation of Automatic Control (IFAC) World Congress; August 28–September 2; Milan. Italy: 2011. pp. 7535-7540

[6] Chen P, Zhang W. Improvement on an inverted decoupling technique for a class of stable linear multivariable processes. ISA Transactions. 2007;**46**(2):199-210. DOI: 10.1016/j.isatra.2006.09.002

[7] Franklin GF, Powell JD, Emami-Naeini A. Feedback Control of Dynamic Systems. 7th ed. London: Pearson Education Limited; 2014. 860 p. DOI: ISBN-10: 0133496597. ISBN-13: 978-0133496598

[8] Corriou JP. Process Control: Theory and Applications. 2nd ed. Switzerland (Cham): Springer International Publishing AG; 2018. 860 p. ISBN-13: 978-3319611433

[9] Kadlec P, Gabrys B, Strandt S. Data-driven soft sensors in the process industry. Computers & Chemical Engineering. 2009;**33**(4):995-814. DOI: 10.1016/j.compchemeng.2008.12.012

[10] Skogestad S, Postlethwaite I. Multivariable Feedback Control: Analysis and Design. 2nd ed. Chichester: John Wiley & Sons, Inc.; 2005. 590 p. DOI: ISBN-10: 0470011688. ISBN-13: 978-0470011683

[11] Albertos P, Sala A. Multivariable Control Systems: An Engineering Approach. 4th ed. London: Springer; 2004. 340 p. DOI: ISBN-10: 1852337389. ISBN-13: 978-1852337384

[12] Gagnon E, Pomerleau A, Desbiens A. Simplified, ideal or inverted decoupling? ISA Transactions. 1998;**37**(4):265-276. DOI: 10.1016/S0019-0578(98)00023-8

[13] Wang QG, Cai WJ, Hang CC. PID control for multivariable processes. Berlin (Heidelberg): Springer Verlag; 2008. 266 p. ISBN-13: 978-3540784821

[14] Melo TR, Silva JJ, Rocha Neto JS. Development of a multivariable control system on an experimental platform dedicated to the study of fouling phenomena. In: Proceedings of the IEEE International Instrumentation and Measurement Technology Conference (I2MTC); 11–14 May; Pisa. Italy: IEEE; 2015. pp. 1314-1319

[15] Barros PR, Campos MCMM, Júnior GA, Carvalho RC d'A, Santos JBM. Application of computer software for system identification and PID control loop tuning to a petrochemical plant. Computer Aided Chemical Engineering. 2009;**27**:693-698. DOI: 10.1016/S1570-7946(09)70336-0

[16] Theil H. Economic Forecasts and Policy. Amsterdam, The Netherlands: North-Holland; 1961. 567 p

[17] Dixon KR. Modeling and Simulation in Ecotoxicology with Applications in MATLAB and Simulink. Lubbock: CRC Press; 2011. 270 p. ISBN-10: 143985517X. ISBN-13: 978-1439855171

[18] Bristol E. On a new measure of interaction for multivariable process control. IEEE Transactions on Automatic Control. 1965;**11**(1):133-134. DOI: 10.1109/TAC.1966.1098266

[19] He M-J, Cai W-J, Ni W, Xie L-H. RNGA based control system configuration for multivariable processes. Journal of Process Control. 2009;**19**(6):1036-1042. DOI: 10.1016/j.jprocont.2009.01.004

[20] Ziegler JG, Nichols NB. Optimum settings for automatic controllers. Transactions of the American Society of Mechanical Engineers (ASME). 1942;**64**(11):759-765

[21] Garcia CE, Morari M. Internal model control. 1. A unifying review and some new results. Industrial & Engineering Chemistry Process Design and Development. 1982;**21**(2):308-323. DOI: 10.1021/i200017a016

[22] Rivera DE, Morari M, Skogestad S. Internal model control. 4. PID controller design. Industrial & Engineering Chemistry Process Design and Development. 1986;**25**(1):252-265. DOI: 10.1021/i200032a041

[23] Melo TR, Silva JJ, Rocha Neto JS. Implementation of a decentralized PID control system on an experimental platform using LabVIEW. IEEE Latin America Transactions. 2017; **15**(2):213-218. DOI: 10.1109/TLA.2017.7854614

[24] Skogestad S. Simple analytic rules for model reduction and PID controller tuning. Journal of Process Control. 2003;**13**(4):291-309. DOI: 10.1016/S0959-1524(02)00062-8

[25] Joseph JB, Brosilow CB. Inferential control of processes: Part I, II and III. American Institute of Chemical Engineering. 1978;**24**(3):485-509. DOI: 10.1002/aic.690240313

[26] Fortuna L, Graziani S, Xibilia MG. Soft Sensor for Monitoring and Control of Industrial Processes. London: Springer; 2007. 271 p. ISBN-10:1846284791. ISBN-13: 978-1846284793

[27] Mansano RK, Godoy EP, Porto AJV. The benefits of soft sensor and multi-rate control for the implementation of wireless networked control systems. Sensors. 2014;**14**(12):24441-24461. DOI: 10.3390/s141224441

[28] Bhuyan M. Intelligent Instrumentation: Principles and Applications. USA: CRC Press; 2011. 524 p. DOI: ISBN-10: 1420089536. ISBN-13: 978-1420089530

[29] Cybenko G. Approximation by superpositions of a sigmoid function. Mathematics of Control Signals and Systems. 1989;**2**(4):303-314. DOI: 10.1007/BF02551274

[30] Wang H, Oh Y, Yoon ES. Strategies for modeling and control of nonlinear chemical processes using neural networks. Computers & Chemical Engineering. 1998;**22**(1):832-862. DOI: 10.1016/S0098-1354(98)00157-4